RSC Advances




ROYAL SOCIETY OF CHEMISTRY

www.rsc.org/advances

Journal Name

ARTICLE

# Hydroconversion of carboxylic acids using mesoporous SBA-15 supported NiMo sulfide catalysts under microwaves

Received 00th January 20xx,
Accepted 00th January 20xx

DOI: 10.1039/x0xx00000x

www.rsc.org/

Titiya Meechai,[a,b] Leclerc Emmanuel,[b] Laurenti Dorothée,[b] Ekasith Somsook,[a] and Geantet Christophe*[b]

Hydrogenation of octanoic acid was performed in a continuous manner, using Microwaves (MW), and a supported metal sulfide catalyst. SBA-15, AlSBA-15 and ZrSBA-15 supported NiMo hydrotreating catalysts were prepared by incipient wetness impregnation method in order to investigate the role of support acidity. Extrudates of the supported NiMo powders were prepared and sulfided. Octanoic acid in dodecane (10%) was introduced in the continuous flow reactor by the mean of an HPLC pump and co-feeded with hydrogen at a working pressure of 0.5 MPa, while varying the reaction parameters such as temperature and feed flow rate (0.1, 0.25, and 0.5 ml/min). The power applied to the monomodal cavity varied in the range of 15-150 W and corresponding temperature from 200-350 °C. Catalysts and supports were characterized by small- and wide-angle XRD, $N_2$-physisorption (BET, BJH), HRTEM, ICP-MS, and $NH_3$-TPD. The thermal response under MW showed that the extrudates containing SBA-15 (with or without Al or Zr) exhibited a strong MW response. The comparison of the catalytic activities showed that all SBA-15 supported NiMo catalysts exhibited the same activity range but the selectivity as compared to $NiMo/Al_2O_3$ catalysts was different.

## 1. Introduction

Despite being an exhaustible fossil resource, crude oil currently remains as the main source of transportation fuels. One alternative is provided by biofuels and more specifically for diesel by the transesterification of vegetable oils. However, biodiesel has some drawbacks such as a limited content in conventional gas oil, a smaller heating value … For these reasons, biodiesel is not fully compatible with existing diesel engines and it is commercialized as a mixture with conventional diesel.[1, 2] In order to circumvent these drawbacks, vegetable oil can be hydrotreated (so called green diesel) to eliminate the oxygen and yield a renewable fuel with features similar to conventional diesel.[3-5] Hydrodeoxygenation (HDO) of triglycerides leads first to the formation of carboxylic acids. Their conversion proceeds on conventional hydrotreating catalysts by three general routes that consist of ketonization, hydrogenolysis and decomposition (decarboxylation and decarbonylation). On sulphide catalysts, hydrogenation steps have been clearly identified with the help of theoretical modelling but the decomposition routes remains unclear.[6, 7] In the field of HDT catalysis, support effect are known to affect performances, dispersion, active phase and reaction pathways.[8] Among alternative supports to conventional alumina, SBA 15 mesostructured support exhibit large pores and its acidity can offer the possibility to tailor the acidity by introducing substituting elements. Therefore, SBA-15 has been studied as support for NiMo hydrotreating catalysts by various researchers.[9-13] The important modification included the incorporation of heteroatoms such as Ti, Zr, and Al in the framework of SBA-15,[14, 15] modifying acidity, texture, and dielectric properties. Hydrotreating properties of such modified SBA-15 have been also investigated.[16-20] It is generally considered that by improving the acidity, hydrotreating performances are improved. The weak interaction between silica and molybdenum results in lower dispersion and higher stacking of the lamellar active phase, which in some cases may benefit to catalytic activity.[21] Hence, in the present study, we investigated the hydrotreating of octanoic acid, under MW, in a fixed-bed reactor using NiMo on SBA-15, ZrSBA-15, and AlSBA-15 catalysts. Whereas the internal temperature distribution of a material subject to conventional heating is limited by its thermal conductivity, with MW, the heating is introduced into the sample from the liquid to the surface of the catalysts. In contrast, microwave heating results in each element of the material being heated individually and selectively, in our case the catalysts itself is heated selectively.[22] The mesoporous properties of SBA15 could be helpful for trapping the reactant closer to the catalyst. Therefore, microwaves heating brings a larger temperature gradient between catalyst and surrounding species leading to acceleration of desorption and species transport in the system.[23-25]

[a] NANOCAST Laboratory, Center for Catalysis, Department of Chemistry and Center of Excellence for Innovation in Chemistry, Faculty of Science, Mahidol University, 272 Rama VI Rd., Thung Phaya Thai, Ratchathewi, Bangkok 10400, Thailand.
[b] IRCELYON UMR 5256 CNRS Université Lyon 1, 2 Av A Einstein 69626, Villeurbanne Cedex, France.

† Footnotes relating to the title and/or authors should appear here.
Electronic Supplementary Information (ESI) available: [details of any supplementary information available should be included here]. See DOI: 10.1039/x0xx00000x

## 2. Material and methods

### 2.1 Materials experimental

P123 ($EO_{20}PO_{70}EO_{20}$, BASF, Mw = 5800), TEOS (tetraethyl orthosilicate), aluminum iso-propoxide, zirconyl chloride, boehmite, ammonium heptamolybdate, nickel nitrate, octanoic acid, dodecane, hexadecane were purchased from Sigma Aldrich and used without further purification.

### 2.2 Support Preparation

The SBA-15 was synthesized with 4 g of P123 that was dissolved in the solution of deionized water and 4 mol/L of HCl. it was stirred at 40°C for 2 h and then 8.5 g of TEOS was slowly added and stirred at 40°C for 20 h. The gel mixture was transferred into a Teflon bottle and aged at 100 °C for 24 h. After that the sample was calcined at 550 °C for 6 h.[19, 26-28]

The Zr-SBA-15 was prepared in the absence of HCl and using $ZrOCl_2.8H_2O$ as zirconium precursor with the same procedure used for SBA-15, but was aged at 100 °C for 2 days.[29-31]

To get Al-SBA-15, P123 was added to 30 mL of water. After stirring for few hours, a clear solution was obtained. Thereafter, aluminium iso-propoxide and the required amount of HCl (pH=1.5) were added, and the solution was stirred at 40 °C for another 2 h. Then, 8.5 g of TEOS was added dropwise with vigorous stirring at 40 °C for 24 h to get a gel and finally crystallized in a Teflon-lined autoclave at 100 °C for 2 days. The crystals were filtered off, dried and calcined in air at 550 °C for 6 h.[32, 33]

### 2.3 Catalyst Preparation

All the catalysts were prepared by standard incipient wetness impregnation (IWI) technique. Molybdenum and nickel precursor salts solutions, with appropriate concentration, were impregnated on the supports. After each impregnation, the catalysts were dried at room temperature for 24 h and at 100 °C for 24 h and then calcined at 500 °C for 5 h.[9, 11, 17, 18, 30, 31, 34, 35]

Extrudates were obtained by mixing 3 g of boehmite AlOOH (binder) with 1 g of each catalyst, and nitric acid. This mixture was carefully mixed and then extruded with a syringe, dried and calcined under air at 500°C for 2 h. The nomenclature Ex- will be used for these various extrudates.

Al content was kept low in order to promote slightly the acidicity, since higher loading (Si/Al 5 or10) were found to induce a severe cracking in the conversion methyl stearate on NiMo supported AlSBA-15 catalysts.[36]

**Table 1** Metal loading and dopants on SBA-15 based catalysts (from chemical analysis)

| Catalysts | Ni (%wt) | Mo (%wt) | Zr or Al (%wt) |
|---|---|---|---|
| NiMo/SBA-15 | 2.54 | 13.49 | |
| Ex-NiMo/SBA-15 | 0.75 | 4.10 | |
| NiMo/Zr-SBA-15 | 2.11 | 11.35 | Zr=6.4 |
| Ex-NiMo/Zr-SBA-15 | 0.71 | 3.94 | |
| NiMo/Al-SBA-15 | 1.99 | 10.79 | Al=0.16 |
| Ex-NiMo/Al-SBA-15 | 0.73 | 4.09 | |
| $NiMo/Al_2O_3$ | 3.00 | 14.00 | |

Ammonia TPD measurements were achieved with BELCAT-M apparatus (BEL JAPAN, INC.). 100–200 mg of catalysts were pretreated at the calcination temperature for 1h under He flow (50 $mL.min^{-1}$, NTP). After cooling down to100 ◦C, $NH_3$ was absorbed by flowing the catalysts under 5% $NH_3$ in He for 30 min (30 $mL.min^{-1}$, NTP) followed by He desorption treatment at 100 °C for 15 min to remove physisorbed molecules. The catalysts were then heated under He flow (50 $mL.min^{-1}$, NTP) up to 450°C with a heating rate of 8 $°C.min^{-1}$. Powder X-ray diffraction patterns were achieved on a Bruker D8 Advance A25 diffractometer equipped with a Ni filter (Cu K radiation: 0.154184nm) and a one-dimensional multistrip detector (Lynxeye, 192 channels on 2.95°). Transmission electron microscopy (TEM) was performed using a JEOL 2010 microscope equipped with an EDS LINK-ISIS detector. The accelerating voltage was 200 kV with $LaB_6$ emission current, a point to point resolution of 0.19 nm. A few mg of the samples, ultrasonically dispersed in an ethanol suspension, were deposited on a holey carbon copper grid.

### 2.4 Hydrodeoxygenation (HDO) in fixed-bed reactor under single-mode MW

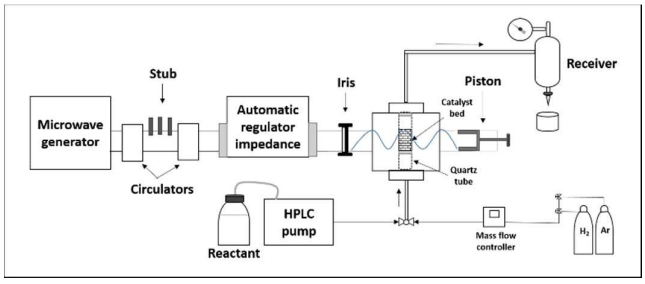


**Scheme 1:** Microwave fixed bed reactor setup

A monomodal cavity has been designed to perform HDO reaction, under $H_2$ pressure, in a continuous manner. The apparatus consists of a generator (2kW, 2.45 GHz Muegge magnetron), circulators, a Tristan automatic tuning system ( Muegge, HOMER$^{HM}$ software) linked to an adapted waveguide resonant cavity equipped with an

iris (I) and plunger (P) close to the system described by Siores et al. or Suttisawat et al.[37] Temperature was measured with a pyrometer focused on the reactor (Raytek). The cylindrical volume of the quartz reactor interacting with the MW in the optimized position of I and P for getting the maximum energy in the reactor filled with 3 g of sulfided NiMo/SBA-15 hydrotreating catalyst extrudates deposited on a quartz frit (volume 24 $cm^3$). Response to MW excitation of the supports oxide catalysts and sulfide catalysts was investigated by 10 Watts increments of input energy after stabilization of the temperature. Octanoic acid (OA) in dodecane (10%) was introduced in the continuous flow reactor by the mean of an HPLC pump and co-feeded with hydrogen under 0.5 MPa of pressure. Power applied to the cavity varies in the range of 15-150 W and corresponding temperature from 200-350 °C depending on the nature of the solid. Various flow rates (0.1, 0.25, and 0.5 ml/min) were also used. Under these conditions, the octanoic acid was converted and reactant and hydrogenation products were analyzed by GC-FID (HP 5890, CPSil5 column 50 m, 0.32 mm, 5µm).

## 3. Results and Discussion

### 3.1 Thermal response of supports and catalysts

The thermal response of the catalytic solids to MW irradiation is given in Figure 1. The benefit of a monomodal cavity is to concentrate the energy on the catalyst in the reactor section localized in the cavity. These preliminary experiments are also required in order to check if any thermal "runaway" cannot be reached under reaction conditions. The supports alone and catalysts under their oxide and sulfide form were first investigated in powder form. The thermal response is linked to electric permittivity, with ε' which characterizes the ability to propagate microwaves into the material and ε'' (imaginary part) which reflects the ability of material to dissipate the energy. The loss tangent tan$\delta$ defined as the ration of these two parameters is also commonly used to describe the losses. The dielectric loss ²Silica based solids are known as poor absorbers, alumina slightly better (tan $\delta$ = 0.066) [38] but $MoS_2$ exhibits good adsorption properties (tan $\delta$ = 0.192). In addition dispersion of $MoS_2$ on alumina enhances dielectric properties and dielectric loss tangent (or dissipation factor by a factor higher than 10).[39] This trend is reflected in Figure 1, the dispersion of molybdenum based sulfides at the surface of the catalyst enhances thermal response. This clearly suggests that energy will be preferentially transferred to the active phase.

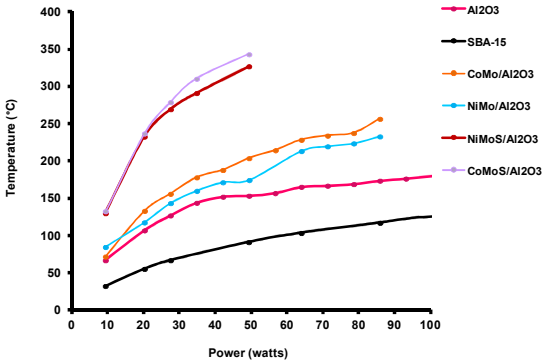


**Figure 1.** Thermal response of MW irradiation in function of the power applied for different supports, oxides and sulfide catalysts.

Concerning the dielectric properties of the extrudates (with about 3 times more alumina than silica based catalyst), the thermal response of the mixture of alumina and catalysts provide a strong response as illustrated by Figure 2. It can be seen that small power inputs on the catalytic extrudates allow reaching easily temperatures in the required range of 200-350°C to proceed to HDO. Due to the relatively low loading incorporated, hetero-atoms (Al, Zr) in the SBA-15 do not drastically modify the dielectric response of the extrudates but all the samples exhibit an almost similar answer to MW excitation, closer than sulfided NiMo/$Al_2O_3$ one .

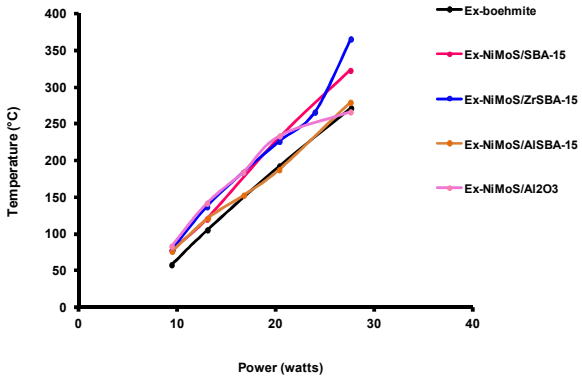


**Figure 2.** Thermal response of MW irradiations from extrudates in the oxidic or sulfide form.

The reactant and solvent themselves exhibit a poor response to microwave excitation at this power range; therefore during the catalytic reaction a temperature gradient occurs in the reactor between the hot surface catalysts and colder reaction mixture.

### 3.2 Characterizations of supports and catalysts

The textural properties of the catalysts and extrudates are given in Table 2. Mesoporous silica exhibit high specific surface

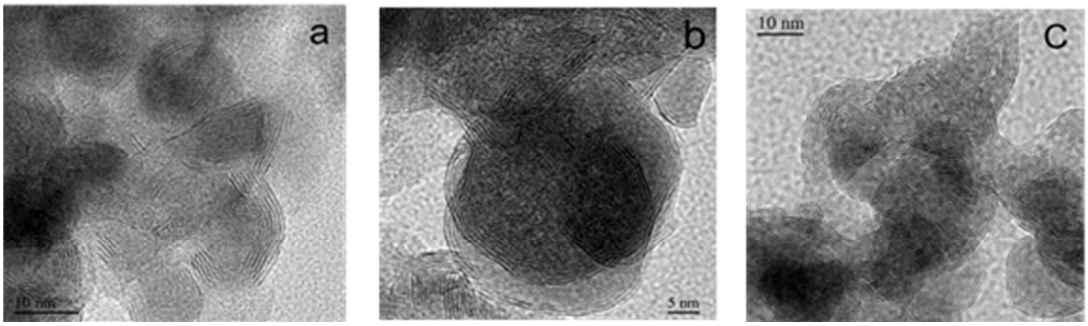


**Figure 3.** HRTEM micrograph for (a) Ex-NiMoS/SBA-15, (b) Ex-NiMoS/ZrSBA-15, (c) Ex-NiMoS/AlSBA-15.

are as strongly reduced by the introduction of the active phase by pore plugging. A narrow distribution of pores with an average porous diameter varying in the range of 5-9 nm is observed for the mesoporous samples and another contribution due to alumina centered at 3.5 nm is observed on the extrudates. Finally, the BET surface area, the pore volume and the average pore diameter of the three extrudates catalysts are very similar.

**Table 2** Textural properties of the supports and catalysts (BET and BJH methods).

| Catalysts | Surface Area, $S_{BET}$ ($m^2$/g) | Pore Volume, Vp ($cm^3$/g) | Average Pore diameter, Dp (nm) |
|---|---|---|---|
| SBA-15 | 958 | 1.34 | 5.6 |
| NiMo/SBA-15 | 434 | 0.85 | 7.9 |
| Ex-NiMo/SBA-15 | 337 | 0.52 | 6.2 |
| Zr-SBA-15 | 728 | 174 | 9.3 |
| NiMo/Zr-SBA-15 | 448 | 1.1 | 8.8 |
| Ex-NiMo/Zr-SBA-15 | 339 | 0.5 | 6.3 |
| Al-SBA-15 | 1098 | 1.26 | 5.7 |
| NiMo/Al-SBA-15 | 508 | 0.72 | 5.7 |
| Ex-NiMo/Al-SBA-15 | 343 | 0.49 | 5.5 |
| NiMo/$Al_2O_3$ | 146 | 0.48 | 2.5 |

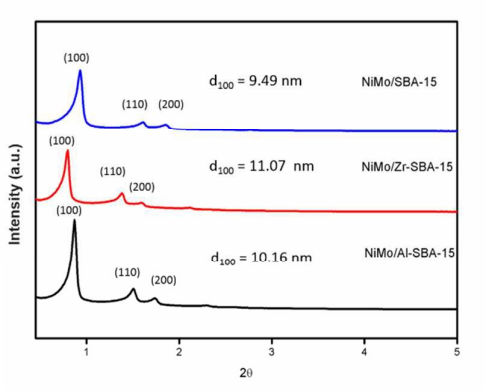


**Figure. 4** Small-angle XRD patterns of NiMo/SBA-15, NiMo/ZrSBA-15, NiMo/AlSBA-15 oxide samples.

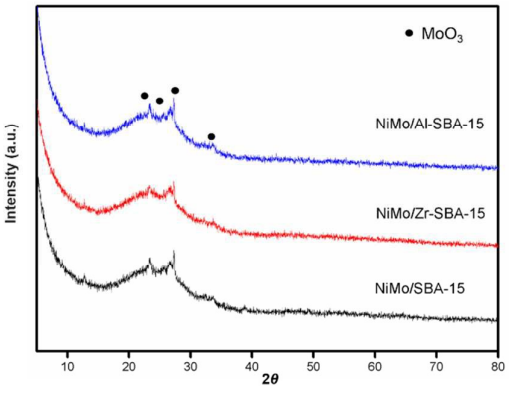


**Figure. 5** Wide-angle XRD patterns of NiMo/SBA-15, NiMo/ZrSBA-15, NiMo/AlSBA-15 oxide samples.

XRD patterns of SBA15 samples NiMo/SBA-15, NiMo/ZrSBA-15, NiMo/AlSBA-15 oxide samples exhibit respectively $d_{100}$ spacing of 9.5, 11 and 10.1 nm characteristic of the organized mesoporous structure (Fig.4).[27, 40, 41] Wide-angle XRD evidences the presence of crystalline $MoO_3$ (black dots in Figure 5.) indicative of the weak

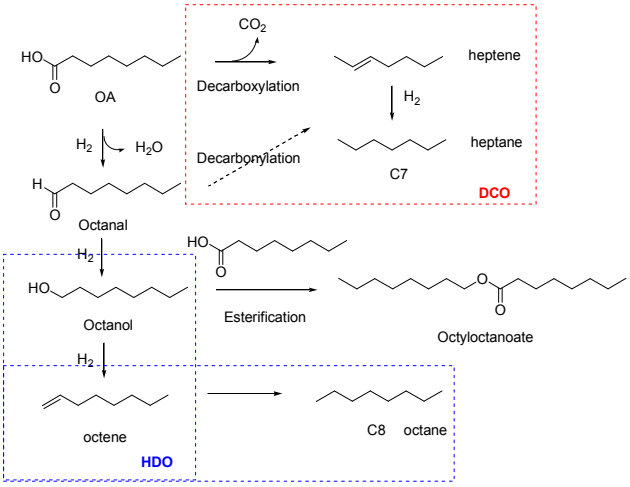


**Scheme 2** : Reaction pathways of octanoic acid (OA) deoxygenation showing the products of DCO and HDO pathways.

interaction of Mo precursors with silica based supports.[30, 35, 42, 43] The active phase of the catalysts is based on lamellar nanocrystallites of $MoS_2$ as illustrated by Figure 3. The distribution of stacking degree and slab length, metal dispersion follows the order ExNiMo/AlSBA-15 > ExNiMo/ZrSBA-15 > ExNiMo/SBA-15 (see Figure 3.). A higher number of $MoS_2$ stacks (average number 6) and a long average slab length (7-17 nm) indicate a poorer dispersion as compared to conventional HDT catalysts.[31]

The acidic properties of the oxidic catalysts were evaluated by ammonia TPD, background corrected and normalized per g of solid spectrum are presented in Fig. 6. The amount of ammonia adsorbed on the surface of NiMoS/SBA-15, NiMoS/ZrSBA-15, NiMoS/AlSBA-15 samples were respectively 258, 394 and 413 µmol/g evidencing that the doping of SBA enhances the amount of acidic sites, even with a low ratio for Al, as it was already reported in the literature.[34, 36, 44]

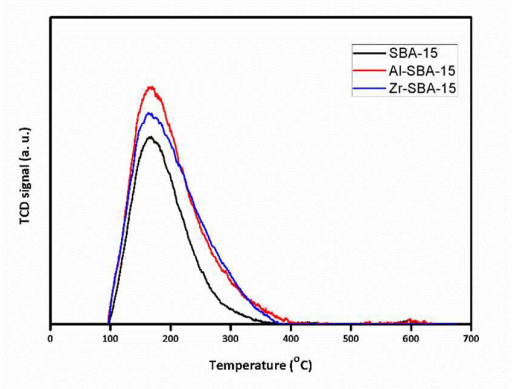


**Figure. 6** Ammonia TPD of SBA-15 based supports.

### 3.3 Catalytic properties

Catalytic properties were investigated by varying reaction temperature, contact time and octanoic acid (OA) concentration. The kinetic order with respect to OA was determined by fitting the kinetic order from the following equation:

$$\frac{1}{n-1}\left(\left(\frac{1}{OA_{out}}\right)^{(n-1)}-\left(\frac{1}{OA_{in}}\right)^{(n-1)}\right)=\frac{k_{app}}{LHSV}$$

with LHSV in $h^{-1}$ and OA input and output concentrations. n was found to be in the range of 2.5-3 (see Figure 7.) indicating complex mechanisms and a strong disparity in the rate constants of the different reaction pathways (DCO versus HDO). At 330°C, all the catalysts have almost the same apparent rate constant close to $k_{app}$ : $1.mmol^2.g^{-2}.h^{-1}$ except Ex-NiMoS/AlSBA-15 which is two times less active as it can be seen on Table 3.

**Table 3** Apparent rate constants of the conversion of octanoic acid with NiMo supported catalysts.

| Catalysts | Rate constants: $K_{app}$ ($1.mmol^2.g^{-2}.h^{-1}$) | |
|---|---|---|
| | 330 °C | 350 °C |
| Ex-NiMo/SBA-15 | 1.1 | 1.8 |
| Ex-NiMo/Zr-SBA-15 | 1.3 | 2.5 |
| Ex-NiMo/Al-SBA-15 | 0.2 | 1.2 |
| Ex-NiMo/$Al_2O_3$ | 1.4 | 3.2 |

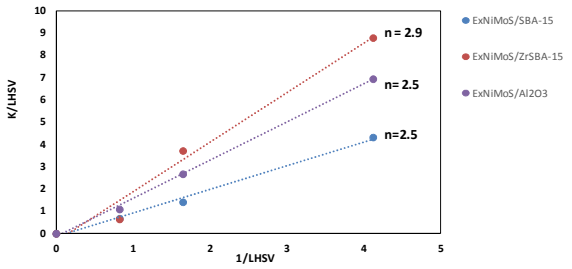


**Figure 7.** Kinetic order determination at different LHSV for ExNiMoS/SBA-15, ExNiMoS/ZrSBA-15, ExNiMoS/AlSBA-15 and ExNiMoS/$Al_2O_3$ catalysts at 350˚C.

In fact, the hydroconversion of OA proceeds via two main well-known pathways: the HDO route which lead to C8 deoxygenated products via hydrogenation/hydrogenolysis reactions, and the DCO pathway which involves decarboxylation/decarbonylation reaction and lead to C7 deoxygenation products. Intermediates like octanal, octanol are also observed as well as esterification products like octyloctanoate (Scheme 2).

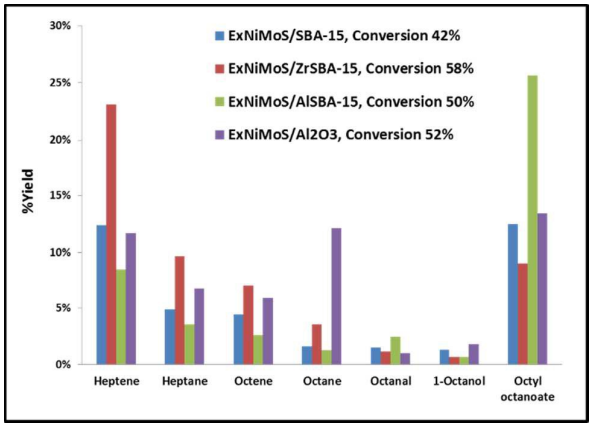


**Figure 8.** Products yields obtained for OA HDO over supported NiMo hydrotreating catalysts at 350°C (catalyst = 3g, Flow rate = 0.25mL/min, P = 0.5 MPa, and $[OA]_o$ = 0.7 mmol/g).

The use of different supports may provide improved activities or different selectivities. Figure 8 illustrates the selectivity observed with the different catalysts at a close level of conversion. The occurrence of the HDO pathway compared to DCO (decarboxylation/decarbonylation) route can be seen by looking at the C8/C7 ratios which include only alkenes and alkanes. The C8/C7 ratio is close to 0.4 for all based SBA-15 catalysts whereas it reached 1.6 for the NiMo on alumina catalyst. This result suggests that the NiMo catalyst supported on alumina favored the HDO pathway and on the contrary the NiMo catalysts supported on SBA-15, modified or not by Al or Zr, lead to the DCO route. In addition, Al containing SBA-15 supported NiMo exhibited a higher yield of octyloctanoate coming from esterification between octanol and OA, compared to the other catalysts, suggesting a contribution of stronger acid sites responsible of the undesired condensation reaction.

## 4. Conclusions

This work illustrates the possibility to use MW activation under continuous flow and pressure conditions to convert octanoic acid, a model of the main intermediate of triglyceride hydrogenation. A low energy input (# 50 W) enables to carry out the conversion in temperature range similar to those used in industrial thermal processes. Even if the dispersion of sulfide catalysts is worth than the one obtained on alumina, by using SBA-15, the catalytic activities remain close to that of a reference catalyst. SBA-15 based catalyst provided a favored route with respect to decarboxylation as compared to NiMo on alumina catalyst. However, a higher acidity obtained by Al substitution in SBA-15 is unfavorable since it promotes the esterification route.

## Acknowledgements

The financial supports by Center of Excellence for Innovation in Chemistry (PERCH-CIC), Royal Golden Jubilee Ph.D. Program (Grant No. PHD/0094/2552) to the PhD student 3.II.MU./52/AN.1, and the Institute of Researches on Catalysis and Environment in Lyon (IRCELYON) are acknowledged. J. F. Rochas from CETIAT and Total are acknowledged for their help and support for setting MW reactor.

## References

1. J. Mikulec, J. Cvengroš, Ľ. Joríková, M. Banič and A. Kleinová, *Journal of Cleaner Production*, 2010, **18**, 917-926.
2. J. C. Serrano-Ruiz, E. V. Ramos-Fernandez and A. Sepulveda-Escribano, *Energy & Environmental Science*, 2012, **5**, 5638-5652.
3. M. Snåre, I. Kubičková, P. Mäki-Arvela, K. Eränen and D. Y. Murzin, *Industrial & Engineering Chemistry Research*, 2006, **45**, 5708-5715.
4. P. Šimáček, D. Kubička, G. Šebor and M. Pospíšil, *Fuel*, 2010, **89**, 611-615.
5. G. W. Huber and A. Corma, *Angewandte Chemie International Edition*, 2007, **46**, 7184-7201.
6. C. Dupont, R. Lemeur, A. Daudin and P. Raybaud, *Journal of Catalysis*, 2011, **279**, 276-286.
7. M. Ruinart de Brimont, C. Dupont, A. Daudin, C. Geantet and P. Raybaud, *Journal of Catalysis*, 2012, **286**, 153-164.
8. M. Breysse, P. Afanasiev, C. Geantet and M. Vrinat, *Catalysis Today*, 2003, **86**, 5-16.
9. S. Badoga, K. C. Mouli, K. K. Soni, A. K. Dalai and J. Adjaye, *Applied Catalysis B: Environmental*, 2012, **125**, 67-84.
10. G. M. Dhar, G. M. Kumaran, M. Kumar, K. S. Rawat, L. D. Sharma, B. D. Raju and K. S. R. Rao, *Catalysis Today*, 2005, **99**, 309-314.
11. P. Rayo, M. S. Rana, J. Ramírez, J. Ancheyta and A. Aguilar-Elguézabal, *Catalysis Today*, 2008, **130**, 283-291.

12. P. Rayo, J. Ramírez, M. S. Rana, J. Ancheyta and A. Aguilar-Elguézabal, *Industrial & Engineering Chemistry Research*, 2008, **48**, 1242-1248.
13. K. Soni, K. C. Mouli, A. K. Dalai and J. Adjaye, *Catal Lett*, 2010, **136**, 116-125.
14. T. Klimova, L. Peña, L. Lizama, C. Salcedo and O. Y. Gutiérrez, *Industrial & Engineering Chemistry Research*, 2008, **48**, 1126-1133.
15. L. Lizama and T. Klimova, *J Mater Sci*, 2009, **44**, 6617-6628.
16. A. Romero-Pérez, A. Infantes-Molina, E. Rodríguez-Castellón and A. Jiménez-López, *Applied Catalysis B: Environmental*, 2010, **97**, 257-268.
17. K. Chandra Mouli, K. Soni, A. Dalai and J. Adjaye, *Applied Catalysis A: General*, 2011, **404**, 21-29.
18. V. Sundaramurthy, I. Eswaramoorthi, A. K. Dalai and J. Adjaye, *Microporous and Mesoporous Materials*, 2008, **111**, 560-568.
19. D. Valencia and T. Klimova, *Catalysis Today*, 2011, **166**, 91-101.
20. S. Badoga, R. V. Sharma, A. K. Dalai and J. Adjaye, *Fuel*, 2014, **128**, 30-38.
21. E. J. M. Hensen, P. J. Kooyman, Y. van der Meer, A. M. van der Kraan, V. H. J. de Beer, J. A. R. van Veen and R. A. van Santen, *Journal of Catalysis*, 2001, **199**, 224-235.
22. G. Roussy, J. A. Pearce in Foundations and industiral applications of microwaves and radio frequency fields. John Wiley &Sons 1995.
23. Y. Suttisawat, H. Sakai, M. Abe, P. Rangsunvigit and S. Horikoshi, *International Journal of Hydrogen Energy*, 2012, **37**, 3242-3250.
24. Z. Chemat-Djenni, B. Hamada and F. Chemat, *Molecules*, 2007, **12**, 1399-1409.
25. S. Horikoshi and N. Serpone, *Catal Sci Technol*, 2014, **4**, 1197-1210.
26. T. Huang, W. Huang, J. Huang and P. Ji, *Fuel Processing Technology*, 2011, **92**, 1868-1875.
27. D. Zhao, J. Feng, Q. Huo, N. Melosh, G. H. Fredrickson, B. F. Chmelka and G. D. Stucky, *Science*, 1998, **279**, 548-552.
28. C. Ochoa-Hernández, Y. Yang, P. Pizarro, V. A. de la Peña O'Shea, J. M. Coronado and D. P. Serrano, *Catalysis Today*, 2013, **210**, 81-88.
29. Y. Du, S. Liu, Y. Zhang, F. Nawaz, Y. Ji and F.-S. Xiao, *Microporous and Mesoporous Materials*, 2009, **121**, 185-193.
30. K. Chandra Mouli, S. Mohanty, Y. Hu, A. Dalai and J. Adjaye, *Catalysis Today*, 2013, **207**, 133-144.
31. S. Badoga, A. K. Dalai, J. Adjaye and Y. Hu, *Industrial & Engineering Chemistry Research*, 2014, **53**, 2137-2156.
32. S. Wu, Y. Han, Y.-C. Zou, J.-W. Song, L. Zhao, Y. Di, S.-Z. Liu and F.-S. Xiao, *Chemistry of Materials*, 2004, **16**, 486-492.
33. P. Bhange, D. S. Bhange, S. Pradhan and V. Ramaswamy, *Applied Catalysis A: General*, 2011, **400**, 176-184.
34. T. E. Klimova, D. Valencia, J. A. Mendoza-Nieto and P. Hernández-Hipólito, *Journal of Catalysis*, 2013, **304**, 29-46.
35. D. Zhang, A. Duan, Z. Zhao, X. Wang, G. Jiang, J. Liu, C. Wang and M. Jin, *Catalysis Today*, 2011, **175**, 477-484.
36. E. W. Qian, N. Chen and S. Gong, *Journal of Molecular Catalysis A: Chemical*, 2014, **387**, 76-85.
37. E. Siores and D. Do Rego, *Journal of Materials Processing Technology*, 1995, **48**, 619-625.
38. A. R. von Hippel, Dielectric materials and applications, John Wiley & Sons, New York 1954.
39. X. Zhang, D. O. Hayward and D. Michael P. Mingos, *Chemical Communications*, 1999, DOI: 10.1039/A901245A, 975-976.
40. A. Corma, M. S. Grande, V. Gonzalez-Alfaro and A. V. Orchilles, *Journal of Catalysis*, 1996, **159**, 375-382.
41. J. P. Dacquin, A. F. Lee, C. Pirez and K. Wilson, *Chemical Communications*, 2012, **48**, 212-214.
42. O. Y. Gutiérrez, K. A. Romero, G. A. Fuentes and T. Klimova, in *Studies in Surface Science and Catalysis*, eds. M. D. D. E. D. V. S. H. P. A. J. J. A. M. E.M. Gaigneaux and P. Ruiz, Elsevier, 2006, vol. Volume 162, pp. 355-362.
43. O. Y. Gutiérrez, D. Valencia, G. A. Fuentes and T. Klimova, *Journal of Catalysis*, 2007, **249**, 140-153.
44. S. Zeng, J. Blanchard, M. Breysse, Y. Shi, X. Shu, H. Nie and D. Li, *Microporous and Mesoporous Materials*, 2005, **85**, 297-304.